

# **Analysis of Combustion products by Time of Flight Mass Spectrometry**

Marina Panariello<sup>1\*</sup>, Barbara Apicella<sup>2</sup>, Mario Armenante<sup>3</sup>, Annalisa Bruno<sup>1</sup>, Nicola Spinelli<sup>1</sup>

<sup>1</sup>CNISM and Dipartimento di Scienze Fisiche, Università di Napoli Federico II, Napoli 80126, Italy

<sup>2</sup>Istituto di Ricerche sulla Combustione – C.N.R., Napoli, Italy

<sup>3</sup>Istituto Nazionale di Fisica Nucleare, Sezione di Napoli, Napoli 80126, Italy

In this work we present a new Time of Flight Mass Spectrometer (TOFMS) for on-line detection of combustion products. The products of a premixed laminar ethylene/oxygen flame at atmospheric pressure were sampled, diluted with inert gas and carried to the ion source as a molecular beam under minimal perturbation. Photoionization has been achieved with laser radiation from a Nd:YAG nanosecond laser at two different wavelengths in the UV range (266nm, 355nm). Also Electron impact ionization (EI) has been employed. The mass spectra obtained using laser wavelength of 355 nm present a mass series of peaks regularly spaced 18 Th up to two thousands of mass unit. This series allowed a precise calibration of the apparatus for high molecular weights. The mass spectra obtained using EI and wavelength of 266 nm allow to detect complex polycyclic aromatic hydrocarbons (PAH) sequences. Information on the ionization efficiency of analyzed species has been obtained by comparing mass spectra produced with different ionization methods.

## **1. Introduction**

The high concentration of organic aerosols in the urban atmosphere is decisively influenced by the carbonaceous species emissions from combustion sources. These constitute a very serious risk for public health and global climatic change. Their complete formation mechanism in combustion systems is still question under debate. There is a constant need of new and more sophisticated instrumentation in order to address these complex problems.

The organic emission of combustion systems is mainly constituted by light hydrocarbons, PAH, organic particulate and soot particles, which cover a largely extended molecular mass range. PAHs are widely accepted to be the chemical precursors to soot. They constitute the building blocks for the growth processes which lead to the formation of high molecular mass structures.

So far, a complete characterization of the all formed chemical species are not yet achieved. Therefore, the development of more advanced investigation methods represents a big challenge in the combustion research activity.

The structural characterization of the chemical species formed in combustion processes depends on progress of specific diagnostic methods as more suitable for the analysis of

carbonaceous structures at different mass range scales. So, different experimental techniques have been adopted for the chemical analysis of PAH and soot aggregates, as Gas Chromatography Mass Spectrometry (Bockhorn et al., 1983; Ciajolo et al., 1982; Ciajolo et al., 2001), Light Scattering, UV-visible absorption and fluorescence (Tregrossi et al., 1997). On-line TOFMS has been successfully applied to low-pressure flames (Keller et al., 2000; Kovacz et al., 1994; Homann and Wolf, 1983) but only few works have been dedicated to TOFMS applied on-line to flame at atmospheric pressure (Hepp et al., 1995; Siegmann et al., 1995).

In this work, a new Time of Flight Mass Spectrometer (TOFMS) for on-line detection at atmospheric pressure of combustion products from small gaseous species up to PAH (MW 400) is described. The main advantage of diagnostic tools operating at atmospheric pressure is the possibility of application to real combustion systems, as engine or industrial plant exhausts.

Different ionization sources, from hard ionization (EI) to soft ionization (UV laser light) have been used and compared in order to study the influence of the ionization processes on combustion products mass spectra. A quantitative analysis has been performed to investigate also the dependence from different combustion conditions.

## 2. Experimental

### 2.1 Set-up

In Fig. 1 the entire experimental apparatus scheme is shown. The TOFMS apparatus scheme is composed by: i) a combustion system, ii) a sampling probe and a transfer line, iii) a supersonic molecular beam, iv) a reflectron TOFMS (Kaesdorf s.r.l) where it is possible to use different types of ionization.

An ethylene-oxygen premixed laminar flame has been produced on a McKenna burner consisting of a water-cooled porous sintered bronze plug of 60 mm diameter. The flame is stabilized with a stainless steel plate ( $d=60$  mm) at 30 mm height above the burner, to obtain a cylindrical flame. A hole in the center of the plate allows the positioning of the sampling probe. Premixed flames are widely employed as controlled experimental models of real combustion systems, because it is possible to monitor the main combustion parameters (fuel/oxygen values, temperature, residence time) and perform studies of reaction kinetic. The burner can be translated allowing the sampling at different positions in the flame. The flame gas sampling is accomplished with a water-cooled stainless-steel probe connected to a suction pump. Flow rates of gases and gas-phase fuel ( $C_2H_4$ ,  $O_2$ ) are controlled with mass flow controllers (Bronkhorst Inc.)

To avoid condensation inside the probe and the transfer line, the sampled gases are diluted within the probe by fluxing an inert gas (Argon) in the inner jacket of the probe. The pumping rate is controlled in order to realize isokinetic conditions (dilution ratio = 50/1, isokinetic suction velocity = 0.29 L/min), corresponding to a minimal perturbation of the flux velocity in the flame.

The sampled gases enter the first chamber of the TOFMS system through a solenoid actuated valve (*General Valve Corporation*, Fairfield NJ, USA, Pulse Valve Series 99) equipped with a 0.8 mm aperture nozzle generating a pulsed supersonic jet. The central part of the jet is extracted by a skimmer to realise a pulsed molecular beam.

The main characteristics on the TOFMS can be summarized as follows: i) 1 m total flight tube length; ii) possibility of switching between positive and negative ions detection; iii) possibility of switching the ionizing source to use alternatively electron

impact, laser radiation or other ionizing sources; iv) two stage ions reflectron region, composed by two grids system, in order to reach a high temporal resolution ( $T/\Delta T = 10,000$ ); v) high detection efficiency for masses of high MW ( $m/z$  up to 100,000 Th); this is obtained by using a high voltage post-acceleration (20 kV) and a detector constituted by a three-stage Multi-Channel-Plate (MCP), to provide a signal amplification up to  $10^8$ - $10^9$ ; vi) operation temperature up to 150 °C and operating pressure in the range  $10^{-9}$ -  $10^{-5}$  mbar.

The TOF-MS system can be operated with a mass filter consisting of a pulsed electric field that can be used to deflect the lightest ions. In these conditions, the saturation of MCP due to the very high signals produced by the most abundant light ions is avoided. Measurements presented in this paper were acquired tuning the mass filter to reduce the signal corresponding to values of  $m/z$  lower than 100 Th.

For EI the electrons are produced by a hot tungsten loop filament. We used repetition rate of 100 Hz has been, limited by the maximum pulsed valve frequency, and a pulse duration of 2  $\mu$ s.

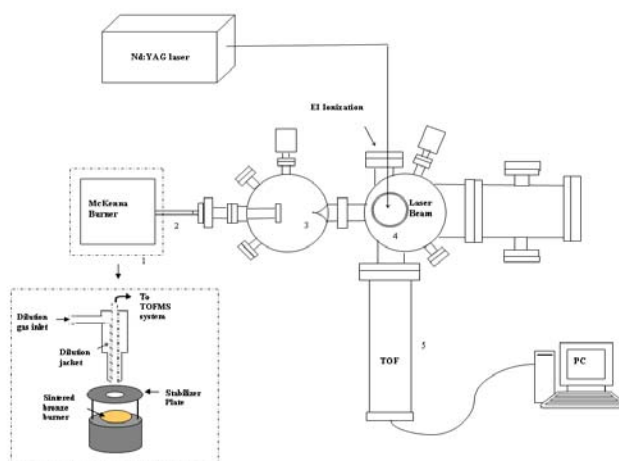


**Fig. 1.** TOFMS apparatus: combustion system (1), sampling probe and transfer line (2), supersonic molecular beam system (3), ionizing chamber (4), Reflectron TOFMS (5). In the inset, the combustion system and the sampling probe are shown with more details.

Photo-ionization has been performed using the 3<sup>th</sup> (355 nm) and the 4<sup>th</sup> (266 nm) harmonics of a Nd:YAG pulsed laser with a repetition rate of 20 Hz and pulse duration of 7 ns. The maximum peak energy was 70 mJ for the 3<sup>th</sup> harmonic and 10 mJ for the 4<sup>th</sup> harmonic. Both harmonics beams have been focused into the ionization chamber by means of a convex lens of 21 cm focal length. The fluence was  $1.7 \times 10^{13}$  W/cm<sup>2</sup> and  $3.2 \times 10^{12}$  W/cm<sup>2</sup> for the 3<sup>th</sup> and the 4<sup>th</sup> harmonics respectively.

## 2.2 Calibration

The time-of-flight measurements allow determining the mass to charge ratio ( $m/z$ ) after a suitable calibration. The following relation links the values of  $m/z$  of the ions and the corresponding time of flight  $t$  (Cotter, 1943):

$$m/z = a + bt + ct^2 \quad (1)$$

where  $a$ ,  $b$  and  $c$  represent three constants depending on the electrical and mechanical characteristics of the mass spectrometer. To determine the three constants, at least 3 reference ions with known masses needs to be identified, preferentially distributed over the whole time-of-flight spectrum to optimize the calibration.

We have first calibrated the TOFMS system with a mixture of noble gases (He, Ar, Xe). The calibration parameters are not enough accurate to analyse spectra containing high molecular weight species, as discussed in more details in a previous work (Panariello et al., 2008). To overcome this problem, bigger ions have to be used as references. If temperature and pressure of sampled gas in the pulsed valve are suitably chosen, the mass spectra obtained with EI and laser ionization  $\lambda=355$  nm show a sequence of regularly spaced peaks extending up to time-of-flight of about 50  $\mu$ s, as reported in Fig. 2.

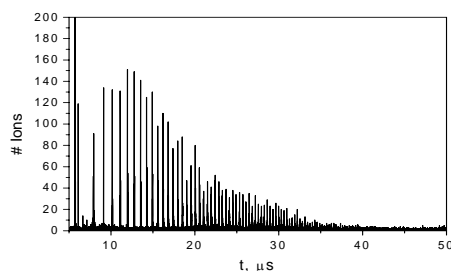


**Fig. 2.** Mass spectrum of combustion products obtained with laser radiation  $\lambda=355$  nm.

A first evaluation of the  $m/z$  distance between two peaks has been determined to be 18 Th. Therefore we have assumed that these peaks correspond to water clusters produced in the expansion process and we used them to obtain a better mass calibration for the entire mass spectral range. We have hypothesized that water clusters are formed from protonated water ( $H_3O^+$ ) produced in flames (Panariello et al, 2008), in agreement with Ledman and Fox (1997) results.

Water clusters peaks represent ideal calibration standards as they are extremely regular and completely free of doubly charged peaks and degradation products that can complicate the calibration process. Moreover, they are formed in controlled conditions inside the chambers. Therefore the calibration can be performed before each set of measurements.

### 3. Results and Discussion

The combustion system was an ethylene/oxygen premixed laminar flame. In this system it is possible to follow the temporal evolution of chemical species as a function of the height above the burner. All the measurements presented here have been performed at 6 mm above the burner surface where the PAHs concentration is maximum.

The flame was operated mainly at a ratio  $C/O=0.65$ , just below the soot formation threshold ( $C/O=0.66$ ; Bohm et al., 1988), for reducing the risk of probe orifice

occlusions by soot, but some measurements has been performed at higher ratio value, in order to study the distribution of masses as function of combustion conditions. All the mass spectra reported have been calibrated as described in the previous section. In Fig. 3 (a) a mass spectrum obtained employing EI with the electrons energy tuned at 70 eV is displayed in terms of the ions detection rate, i.e. the number of detected ions normalized to the number of ionizing pulses. We report the mass spectra starting from  $m/z$  50 Th because below this value the signals are strongly reduced by the mass filter. Strong signals are present in the region of  $m/z$  lower than 100 Th, with a maximum around benzene, followed by decreasing signal intensity up to 200 Th and a new increase around 300 Th. In the expanded region of 120-400 Th of Fig. 3 (b) the typical peaks distribution of PAHs from naphthalene (128 Da) up to ovalene (398 Da) is well visible. Above 400 Th the signal/noise ratio becomes too low for species identification.

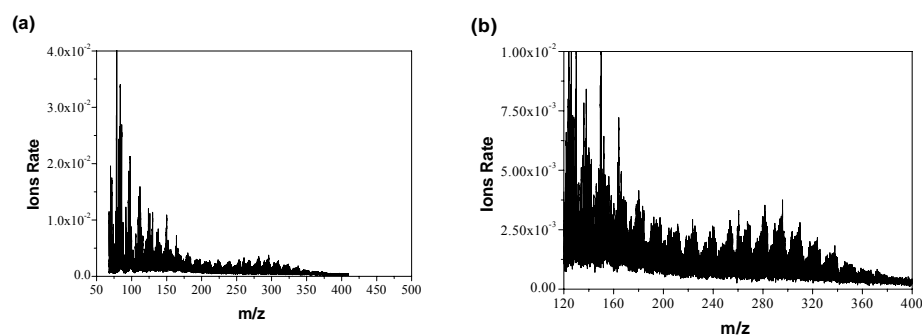


**Fig. 3.** TOFMS spectrum of combustion products acquired with EI (a) and its zoom in the  $m/z$  range 120-400 Th (b).

In Fig. 4 (a) a TOFMS spectrum acquired with laser radiation  $\lambda=355$  nm (laser fluence of  $1.7 \times 10^{13}$  W/cm<sup>2</sup>) is reported with its expanded region in the  $m/z$  range 120-400 Th (Fig. 4 (b)). In this spectrum, the sequence of peaks with gap of 18 Th dominates the PAHs sequence.

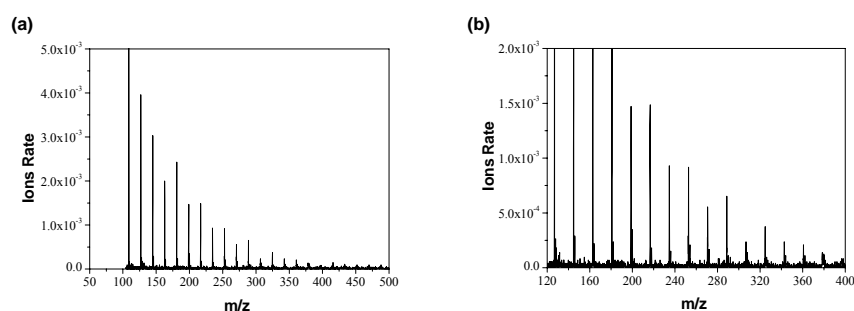


**Fig. 4.** TOFMS spectrum of combustion products acquired with laser light  $\lambda=355$  nm (a) with a zoom of the  $m/z$  range 120-400 Th (b).

In Fig. 5 (a) the mass spectrum at 266 nm (laser fluence is  $3.2 \times 10^{12}$  W/cm<sup>2</sup>) and its zoom of the range of  $m/z$  120-400 Th (Fig. 5 (b)) is reported. It shows a different

distribution of peaks intensities with respect to the one obtained with the EI (Fig. 3), according to the results reported in literature by Happold et al (2007).

In this case, the strongest peaks are around naphthalene (128 Th) and the ions in the mass range between 50-100 Th are less abundant than in the mass spectrum reported in Fig. 3 (a) for the electron ionization. For greater values of  $m/z$  the peak intensity decreases but at this wavelength the minimum in the ions detection rate around 200 Th is not present. Moreover similar sequences of PAH peaks as detected in the case of electron impact has been revealed. As in EI case, the production rate falls down for  $m/z$  larger than 400 Th.

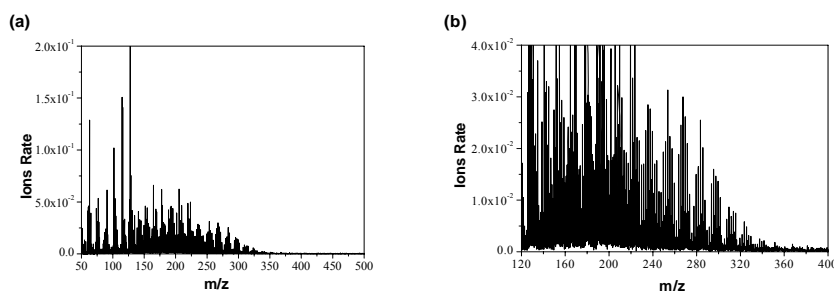


**Fig. 5.** TOFMS spectrum of combustion products with laser light 266 nm (a) and its expanded region in the  $m/z$  range 120-400 Th (b).

A quantitative analysis has been performed employing EI and 266 nm laser ionization sources to compare different ionization methods. The mass spectra have been divided in three masses ranges and the total numbers of ions in each range have been calculated and normalized to the ionizing pulse intensity and repetition rate. The three ranges correspond to  $m/z$ : 50-200, 200-500, >500 Th.

The results for  $C/O=0.65$  flame, using either the electron and 266 nm wavelength have reported in Tab. 1.

It is noteworthy that signal decreases with increasing mass, that is more evident when the EI rather the 266 nm laser ionization is employed. This is due to the different efficiency of the two ionization methods and/or to double ionization and fragmentation processes which are more relevant with EI.

**Tab. 1:** Detected ion rates in different  $m/z$  regions and the ratios between the detected ion rates for  $C/O=0.65$  flame, for different ionization methods.

C/O	Ionization	RateA $m/z < 200$	Rate B $200 < m/z < 500$	RateC $m/z > 500$	A/ B	B/ C
0.65	EI (70eV)	211.19±0.05	15.46±0.02	7.06 ±0.01	13.66±0.06	2.99±0.02
0.65	Laser, $\lambda=266$ nm	0.37±0.08	0.086±0.004	0.036±0.002	4.23±0.01	2.414±0.004

The same analysis has been applied to the mass spectra corresponding to different  $C/O$  ratio. The ions number has been calculated in each mass range, either for EI and 266 nm laser ionization. The detected ions rates in different mass regions and the ratios between them using EI are listed in Tab. 2.

**Tab. 2:** Detected ion rates in different  $m/z$  regions and the ratios between the detected ion rates. These values concern the mass spectra of C/O ratio with EI.

<b>Electron Ionization</b>	<b>C/O</b>	<b>RateA <math>m/z &lt; 200</math></b>	<b>Rate B <math>200 &lt; m/z &lt; 500</math></b>	<b>RateC <math>m/z &gt; 500</math></b>	<b>A/ B</b>	<b>B/ C</b>
EI, 70 eV	0.6	1515.1±0.2	66.20 ±0.05	4.06 ±0.01	22.9±0.2	16.29±0.05
EI, 70 eV	0.65	1550.9±0.2	40.89±0.04	2.43±0.01	37.9±0.2	16.83±0.04
EI, 70 eV	0.7	1396.1±0.2	29.17±0.03	1.92±0.02	47.9±0.2	1.52±0.04

Also in this case, we can observe in each mass range a decrease of detection rate as the mass increases.

For the C/O ratio values 0.6, 0.65 and 0.7, the detected ions Rate A (50-200 Th) does not seem to vary meaningfully, while either the Rate B and the Rate C show a noticeable decrease as the C/O ratio value increases. This can be explained through two possible mechanisms: i) the decrease in the detection of larger PAH ions could probably correspond to formation processes of the nanometric and soot particles ; ii) The decrease of larger PAH ions rate could be related to losses on the sampling probe inner walls. As the C/O ratio grows (richer flames), the high molecular weight organic compounds formation are provided. They could adhere on the probe inner walls, involving as “aggregation seeds” for the larger mass PAHs. The effect is a transport efficiency reduction toward high masses compared low masses PAHs.

The detected ions total number, obtained using the 266 nm laser radiation, is reported in Tab. 3, for the three mass ranges in which the mass spectra have been divided.

With exception of C/O=0.53 flame ratio, where the higher rate value seems corresponding to the intermediate mass range 200-500 Th, for the all C/O flame ratio we can note a decrease of detected ions number as the molecular weight of combustion products increases. Particularly, this decrease is very prompt for C/O=0.65.

**Tab. 3:** Detected ion rates in different  $m/z$  regions and the ratios between them. These values concern the mass spectra for C/O ratio different values, using  $\lambda=266$  nm photo-ionization. The height above the burner for combustion products sampling is  $z=6$ mm.

<b>Photo-Ionization</b>	<b>C/O</b>	<b>Rate A <math>m/z &lt; 200</math></b>	<b>Rate B <math>200 &lt; m/z &lt; 500</math></b>	<b>Rate C <math>m/z &gt; 500</math></b>	<b>A/ B</b>	<b>B/ C</b>
$\lambda=266$ nm	0.53	0.163±0.005	0.194±0.006	0.101±0.004	0.84±0.08	1.922±0.007
$\lambda=266$ nm	0.6	1.82±0.02	1.04±0.01	0.177±0.005	1.75±0.02	5.87±0.01
$\lambda=266$ nm	0.65	7.86±0.04	3.37±0.02	0.191±0.006	2.33±0.04	17.61±0.02
$\lambda=266$ nm	0.7	1.407±0.015	0.89±0.01	0.204±0.006	1.59±0.02	4.34±0.01
$\lambda=266$ nm	0.8	1.25±0.01	0.82±0.01	0.150±0.005	1.53±0.02	5.47±0.01

Moreover, the detected ions Rate B and the detected ions Rate A increase as the C/O ratio increases up to C/O=0.65, but beyond this value, hence above the soot formation threshold, the detected ions rates begin to decrease. This behaviour could indicate an efficiency loss of sampling probe, as just discussed in the previous analysis. In fact, beyond the soot formation threshold (C/O=0.66 ratio value for this flame), particles of

bigger dimensions begin to form, sticking to inner walls of the probe. They behave like aggregation seeds for PAHs of low and intermediate masses. A possible explanation of disagreement for C/O=0.53 flame could be due to very low signal/noise ratio, particularly in the low mass range (50-200 Th).

#### 4. Conclusions

Combustion products mass spectra from a premixed laminar ethylene/oxygen flame have been analyzed in real time by an on-line TOFMS system at atmospheric pressure. EI ( $E=70$  eV) and photo-ionization ( $\lambda=266$  nm;  $\lambda=355$  nm) have been employed. The distribution of PAHs from naphthalene up to ovalene has been achieved. A comparison between the different ionization sources has been performed in order to analyze the influence of the ionization method. The distribution of masses/sizes has been studied as function of the C/O flame ratio. In all cases the detection rate of ions becomes low for  $m/z$  larger than 400 Th.

#### References

- Bockhorn, H., F. Fetting, and H.W. Wenz, 1983, *Ber. Bunsenges. Phys. Chem.* 87, 1067.
- Bohm, H., D. Hesse, H. Jander, B Luers, J. Pietscher, H.G.G. Wagner and M. Weiss, 1988, *Proceedings of The Combustion Institute.* 22, 403-411.
- Ciajolo, A., R. Barbella, M. Mattiello and A. D'Alessio, 1982, *Proceedings of The Combustion Institute.* 19, 1369.
- Ciajolo, A., B. Apicella, R. Barbella, A. Tregrossi, F. Beretta and C. Allouis, 2001, *Energy & Fuel.* 15, 987.
- Cotter, R.J., 1943, *Time-of-flight Mass Spectrometry: Instrumentation and applications in biological research.* ACS, Washington, DC.
- Happold, J., H.H. Grotheer and M. Aigner, 2007, *Rapid. Commun. Mass Spectrom.* 21, 1247.
- Hepp, H., K. Siegmann and K. Sattler, 1995a, *Chem. Phys. Lett.* 233, 16.
- Homann, K.H. and H. Wolf, 1983, *Ber. Bunsenges. Phys. Chem.* 87, 1073.
- Ledman, D.W., and R.O. Fox, 1997, *J. Am. Soc. Mass Spectrom.* 8, 1158.
- Keller, A., R. Kovacs and K.H. Homann, 2000, *Phys. Chem. Chem. Phys.* 2, 1667-1675.
- Kovacz, R., S. Loffler and K.H. Homann, H. Bockhorn, Ed., 1994, *Soot Formation in Combustion.* Springer, Berlin Heidelberg, New York.
- Siegmann, K., H. Hepp and K. Sattler, 1995b, *Combust. Sci. Technol.* 109, 165.
- Panariello, M., B. Apicella, A. Bruno, M. Armenante and N. Spinelli, 2008, *Rapid Commun. Mass Spectrom.* 22, 573.
- Tregrossi A., A. Ciajolo and R. Barbella, 1997, *National Congress of Informatic Chemistry, Napoli, Italy*, p. 295.